CHAPTER II

OPTICAL AND MAGNETIC STUDIES OF DIVALENT $3d^7$ ION DOPED IN $CsCdCl_3$

We have grown large single crystals of both Cr^{3+} and Co^{2+} doped $CsCdCl_3$. But as we are not definite of the valence state of Cr ion in $CsCdCl_3$, we have conducted the measurement on optical and magnetic properties only of the crystal doped with Co, which has been chemically and spectroscopically found to be in divalent state.

RESULTS AND DISCUSSION

I. Optical Studies

The theory of the optical spectra of octahedrally coordinated Co^{2+} ion was worked out by Orgel[24] and Low[36] on the basis of the energy matrices given by Finkelstein and Van Vleck[18] for $3d^3$ or $3d^7$ on the weak field scheme, while Koide[134] and Ferguson, Wood and Knox[102] approached the problem on the strong-field approximation. Tanabe and Sugano[22] also calculated the energy levels of different states of Co^{2+} taking into consideration the various configurational interactions. Theory of electronic properties of $3d^3$ and $3d^7$ trigonal compounds was worked out by Liehr[135] and Perumareddi[136].

The electronic configuration of $3d^7$ of a cobalt ion has ^4F as the lowest level in its free state and the next level

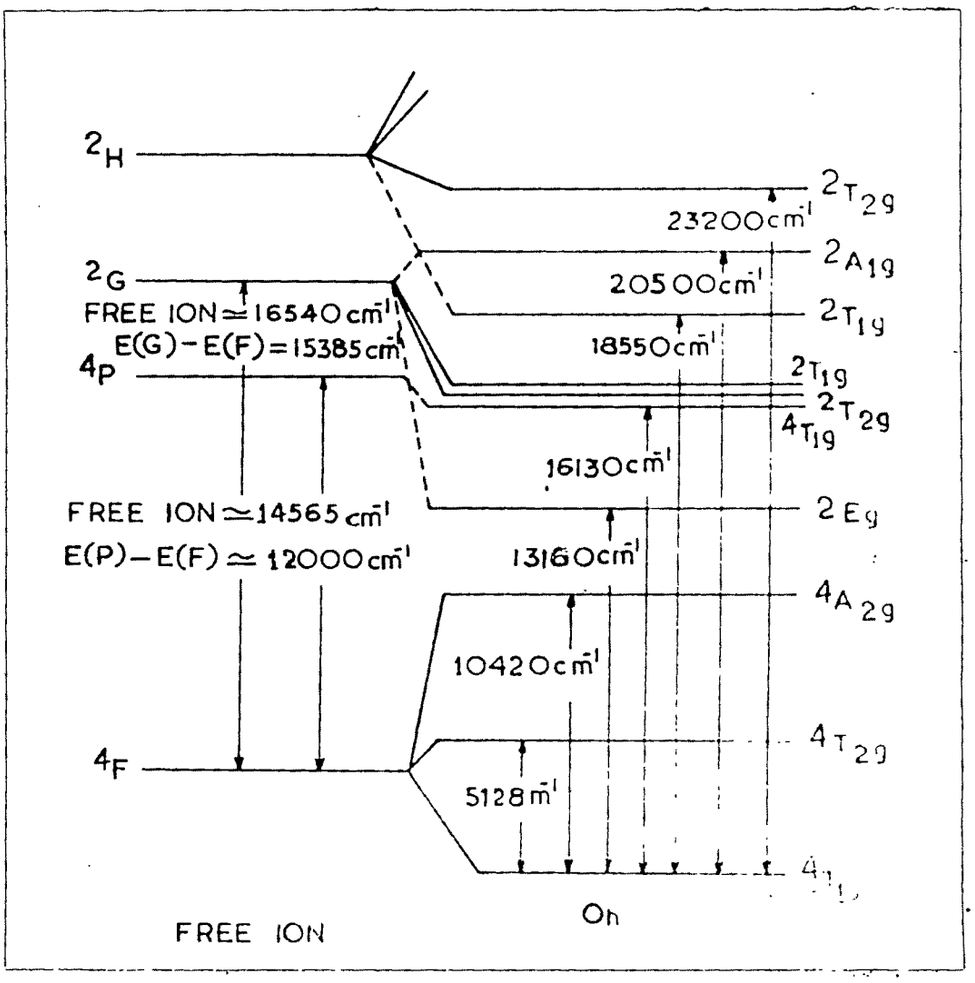

Fig.7a.

Fig.7a. Octahedral energy level scheme of various Stark levels of Co^{2+} in $CsCdCl_3$. The observed separations are indicated by arrows (Not to scale).

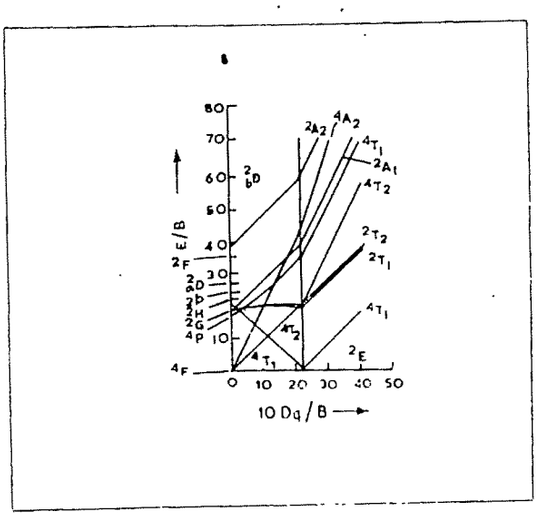

Fig. 7b.

Fig.7b. Tanabe-Sugano energy level diagram for the d^7 configuration[22]

^4P lies at a distance of about 14000 cm^{-1} above the lowest one. Under a crystalline field of O_h symmetry the seven-fold degenerate F-state splits into an one-fold ($^4A_{2g}$) and two three-fold ($^4T_{1g}$ and $^4T_{2g}$) orbitally degenerate levels, with $^4T_{1g}$ lying lowest. The upper ^4P state transforms into $^4T_{1g}$ under cubic point group. The energy level scheme for Co^{2+} under O_h symmetry is shown in Fig. 7a.

A. Broad Features

The energy levels of ions which arise from a fixed number of d-electrons can be described by just two Racah parameters B and C which are related to the Slater integrals F_2 and F_4 of the atomic spectra ($B = F_2 - 5F_4$, $C = 35\ F_4$). The cubic field parameters Dq and the Racah parameter B are sufficient to categorize all the quartet (S = 3/2) state energies of the Co^{2+} ion placed in an octahedral environment. The parameters can be determined from the observed energies for $^4T_{1g} \longrightarrow {}^4T_{2g}$ and $^4T_{1g} \longrightarrow {}^4T_{1g}$ (P) transitions. The energies of the various quartet levels after taking configuration interactions into account are :

$^4T_{1g}$ (P) : $-\frac{1}{2}$ (15B + 6 Dq) + $\frac{1}{2}$ ($225B^2$ + 180 B Dq + $100\ Dq^2$)$^{\frac{1}{2}}$

$^4A_{2g}$ (F) : 12 Dq - 15 B

$^4T_{2g}$ (F) : 2 Dq - 15 B

$^4T_{1g}$ (F) : $-\frac{1}{2}$ (15 B + 6 Dq) - $\frac{1}{2}$ ($225B^2$ + 180 B Dq + $100\ Dq^2$)$^{\frac{1}{2}}$

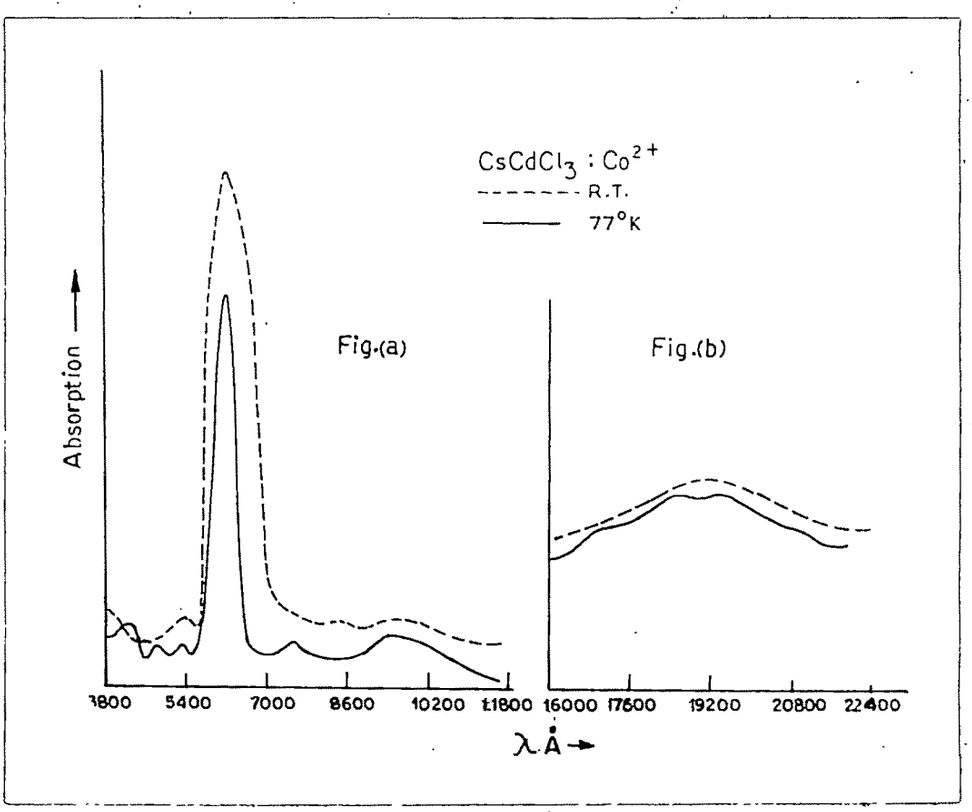

Fig. 8. Absorption spectrum of Co^{2+} in $CsCdCl_3$. The dotted line is the room temperature spectrum and the solid line that taken at 77°K.

Fig. (a) : From 3800 Å to 11800 Å

Fig. (b) : From 16000 Å to 22400 Å (thick crystal)

The transition energies are given by

$$\left[{}^4T_{1g}\ (F) \longrightarrow {}^4T_{2g}^{(F)}\right] \ : \ \nu_1 = 2\ Dq - \tfrac{1}{2}(15B - 6\ Dq) + \tfrac{1}{2}(225B^2 + 180B\ Dq + 100\ Dq^2)^{\frac{1}{2}}$$

$$\left[{}^4T_{1g}\ (F) \longrightarrow {}^4A_{2g}^{(F)}\right] \ : \ \nu_2 = 12\ Dq - \tfrac{1}{2}(15B - 6\ Dq) + \tfrac{1}{2}(225B^2 + 180B\ Dq + 100\ Dq^2)^{\frac{1}{2}}$$

$$\left[{}^4T_{1g}\ (F) \longrightarrow {}^4T_{1g}\ (P)\right] : \nu_3 = (225B^2 + 180B\ Dq + 100\ Dq^2)^{\frac{1}{2}} \qquad (77)$$

From the unpolarized room temperature spectra (Fig. 8 - dotted line) of $CsCdCl_3$: Co^{2+} (2.7 mol %), we ascribe the main absorption band at 16000 cm^{-1} to the ${}^4T_{1g}\ (F) \longrightarrow {}^4T_{1g}\ (P)$ transition (ν_3). The weak broad band in the region 5000 cm^{-1} to 5500 cm^{-1} has been identified as ${}^4T_{1g}\ (F) \longrightarrow {}^4T_{2g}\ (F)$ transition (ν_1). Taking the centre of this broad band at 5130 cm^{-1} and from the above relations (Eqn. 77), the values of Dq and B were found to be $\sim$ 595 cm^{-1} and 780 cm^{-1} respectively. Comparison of this Dq value with that obtained from octahedral Co^{2+} in MgO (960 cm^{-1})[36] and $CoCl_2$ (690 cm^{-1})[102] indicates that our value of Dq is on the low side. The observed Dq is much less than 9/4 of the Dq expected theoretically in the tetrahedral $CoCl_4^{=}$ ion in Cs_3CoCl_5 which is about 325 cm^{-1} [107]. It is to be remembered in this connection that there is a large difference between the ionic radii of Cd^{2+} (0.97 Å)[137] and Co^{2+} (0.72 Å)[138]. It is then obvious that the observed low value of Dq is to be ascribed to (1) much larger Co-Cl distance (Cd-Cl distance $\simeq$ 2.6 Å) in the present case as compared to $\simeq$ 2.2 Å in normal chlorides of Co^{2+},

(2) much weaker ligand as compared to Co^{2+} doped in MgO (Mg - O $\sim$ 2.1 Å)[139]. The value of B on the other hand is close to those of AgCl : Co^{2+} (790 $\pm$ 20 cm^{-1})[104] and $CoCl_2$ (780 cm^{-1})[102] showing that this Racah parameter is not much affected due to change in nature and distance of the ligand. Taking the value of B to be $\sim$ 780 cm^{-1}, the term value, i.e. the energy between ^4F and ^4P, which is 15B is found to be $\sim$ 11700 cm^{-1}. This is less than the free ion value, but greater than that observed in the case of O^{2-} ligand as it should be.

Expressing the coefficient of spherical harmonics Y_4^0, of the octahedral crystalline electric field V_c (Eqn. 11) in terms of the distance R for point charge η from the origin[41]

$$\gamma_4^0 = - \frac{e\eta\sqrt{4\pi}}{R^{4+1}\sqrt{2\times4+1}} \qquad (78)$$

it will be seen that the crystal field strength and hence the parameter Dq roughly varies as $(1/R^5)$. Thus, a 15% increase in bond distance should decrease the Dq by roughly 75%. Also, increasing the ligand charge increases the intensity of the field proportionally. The observed decrease with distance as in above example, however, is much less, indicating that the simple point charge calculation is rather qualitative. If overlap between metal-ligand charge clouds is considered, a much less dependence of Dq on bond-distance is expected and the discrepancy is likely to be removed. Finally Dq may be compared with the value of 380 cm^{-1} found in eight coordinated cube

(CaF_2 : Co^{2+})[140] (bond distance 2.36 Å)[139], which is even less than the present case.

The observed Dq value indicates that Co^{2+} ions replace the Cd^{2+} at predominantly octahedral or distorted octahedral sites in $CsCdCl_3$. This has also been confirmed by our magnetic measurements. This makes the study interesting since most of the halides of Co^{2+} provide tetrahedral fields. With the above value of Dq and B, the transition $^4T_{1g}$ (F) $\longrightarrow$ $^4A_{2g}$ is placed at $\sim$ 11065 cm^{-1}. In Fig. 8 it can be seen that at $\sim$ 10380 cm^{-1} there is an indication of a very weak absorption band. This is confirmed by observation on a crystal with larger path length. This weak absorption band is ascribed to $^4T_{1g}$ (F) $\longrightarrow$ $^4A_{2g}$ (F) transition (ν_2). The relative weakness of this transition can be understood as follows. Expressing all the levels of interest in terms of the t_{2g} and e_g orbitals, the $^4A_{2g}$ state arises from the configuration $t_{2g}^3 e_g^4$ with a small admixture of the $t_{2g}^4 e_g^3$ configuration coming from the ^4P level of the free ion. Such a transition involving the change of two d-orbitals (i.e. a two-electron jump) should be forbidden (for the dipole moment operator is an one-electron operator). The $^4T_{1g} \longrightarrow {}^4A_{2g}$ absorption can be attributed primarily to the admixed component of the upper $^4T_{1g}$ level.

The doublet (S = 1/2) states are shown in Fig. 7a. The states in order of increasing energy separation from the ground state are ^2E_g, $^2T_{2g}$, $^2T_{1g}$, $^2T_{1g}$ and $^2A_{1g}$. Their energies can be obtained by solving the secular equations given by Tanabe and

Sugano matrices for $3d^7$ ion[22]. As the ground state is a quartet, the transition to a doublet involves a change in spin multiplicity and it must proceed via a spin dependent coupling, so we can expect the transition to be weaker than that to the quartet levels.

The sharp band observed at 18400 cm^{-1} (Fig. 8) may be ascribed to the spin forbidden transition to an orbital triplet which arises from either ^2G or ^2H term. The high intensity of this transition is presumably due to mixing with close-lying quartet state. We have examined this state more closely at liquid hydrogen temperature. The best way to prove the spin-forbidden character of the band is, of course, by splitting it under magnetic field, but unfortunately the band-width at 77°K is too large to allow us to study Zeeman effect even with our pulsed field 100 kilogauss magnet. With increase in crystal field, the state ^2E_g, a component of ^2G moves down in energy rather sharply[22] (Fig. 7b) while $^2T_{1g}$ and $^2T_{2g}$ energies are not so sensitive to the crystal field. The small hump at 11770 cm^{-1} (Fig. 8) may be ascribed to $^4T_{1g}$ (F) $\longrightarrow$ ^2E_g transitions.

At 77°K the entire spectrum (Fig. 8 solid line) is found to be shifted towards the shorter wave length side and there is a considerable sharpening of the absorption bands. The position of the main transition band for the ground $^4T_{1g}$ (F) to $^4T_{1g}$ (P) state has shifted from 16000 cm^{-1} to 16130 cm^{-1}.

The first excited state $^4T_{2g}$ (F) which we have observed as a broad band from 5000 cm^{-1} to 5500 cm^{-1} is found to be split up into four components at 5880 cm^{-1}, 5380 cm^{-1}, 5150 cm^{-1} and 4760 cm^{-1}, respectively. The observed splitting may be due to the combination of the small trigonal field and spin-orbit coupling. But as we are unable to observe any polarization effect we could not identify them uniquely. The transition $^4T_{1g}$ (F) $\longrightarrow$ $^4A_{2g}$ (F) at 10380 at room temperature has shifted to 10420 cm^{-1} at liquid nitrogen temperature. In addition to the spin-doublet which has shifted from 18400 cm^{-1} to 18550 cm^{-1}, we have observed new weak absorption bands at 23200 cm^{-1} and 20500 cm^{-1}. The position of the crystal-field-sansitive ^2E_g term is found to be shifted from 11770 cm^{-1} at room temperature to 13160 cm^{-1} at 77^oK.

Ignoring the effect of spin-orbit coupling and varying B and Dq, and assuming C = 5B, we have solved the energy matrices of $3d^7$ ion given by Tanabe and Sugano[22] for different terms with the help of 1130 I.B.M. Computer at the Computation Centre, Calcutta University. The best fit with our observed energies is found to be at Dq = 595 cm^{-1} and B = 800 cm^{-1}. The energies and energy matrices of different terms with above values are given in Table 8. The calculated and observed energies of the states are given in Table 9.

Table 8 : The energies and energy matrices for doublet terms of $CsCdCl_3 : Co^{2+}$ with values of crystal field parameters : Dq = 595 cm^{-1}, B = 800 cm^{-1} and C = 5B (After Tanabe and Sugano, 1954)[22].

Term	Energy (10^{-3} cm^{-1})	$t_2^3(^2T_2)e^4$	$t_2^4(^3T_1)e^3$	$t_2^4(^1T_2)e^3$	$t_2^5(^1A_1)e^2$	$t_2^5e^2(^1E)$
$^2{}_aT_2$	16.53	27140.0	-4156.9	- 6928.2	11200.0	1600.0
$^2{}_bT_2$	22.87	- 4156.9	8390.0	2400.0	- 4156.9	-4156.9
$^2{}_cT_2$	27.46	- 6928.2	2400.0	16390.0	- 1385.6	1385.6
$^2{}_dT_2$	34.72	11200.0	-4156.9	- 1385.6	20040.0	8000.0
$^2{}_eT_2$	55.63	1600.0	-4156.9	1385.6	8000.0	5640.0

Term	Energy (10^{-3}) cm^{-1})	$t_2^3(^2T_1)e^4$	$t_2^4(^3T_1)e^3$	$t_2^4(^1T_2)e^3$	$t_2^5e^2(^3A_2)$	$t_2^5e(^1E)$
$^2{}_aT_1$	16.61	14340.0	-2400.0	2400.0	0.0	-2771.2
$^2{}_bT_1$	18.42	- 2400.0	13190.0	- 2400.0	2400.0	4156.9
$^2{}_cT_1$	24.04	2400.0	-2400.0	8390.0	-2400.0	-4156.9
$^2{}_dT_1$	27.92	0.0	2400.0	- 2400.0	2400.0	2771.2
$^2{}_eT_1$	36.62	-2771.2	4156.9	- 4156.3	2771.2	5640.0

Table 8 (Contd.)

Term	Energy (10^{-3} cm^{-1})	$t_2^3 (^2E) e^4$	$t_2^4 (^1A_1) e^3$	$t_2^4 (^1E) e^3$	$t_2^6 e$
$^2_aE_g$	11.96	14340.0	- 6788.2	- 3394.1	0.0
$^2_bE_g$	25.15	- 6788.2	31590.0	8000.0	9699.4
$^2_cE_g$	28.67	- 3394.1	8000.0	12390.0	2262.7
$^2_dE_g$	55.12	0.0	9699.4	2262.7	-1110.0

Table 9 : Electronic energy levels of Co^{2+} in $CsCdCl_3$ (B = 800 cm^{-1}, Dq = 595 cm^{-1}, C = 5B). All energies are in cm^{-1}

Transitions $^4T_{1g}$ (F) →	Calculated	Observed at 300°K	Observed at 77°K
$^4T_{2g}$ (F)	5125	5000 - 5500	(i) 4760 (ii) 5150 (iii) 5380 (iv) 5880
$^4A_{2g}$ (F)	11065	10380	10420
^2E_g	11962	11770	13160
$^4T_{1g}$ (P)	16280		
$^2_aT_{2g}$	16526	16000	16130
$^2_aT_{1g}$	16612		
$^2_bT_{1g}$	18422	18400	18550
$^2A_{1g}$	20315	-	20500
$^2_bT_{2g}$	22870	-	23200

The lowest two $^2T_{2g}$ spin-doublets are calculated to have energies at 16526 cm^{-1} and 22870 cm^{-1} respectively. The first position is very close to the main absorption band $^4T_{1g}$ (F) $\longrightarrow$ $^4T_{1g}$ (F) at 16000 cm^{-1} and thus might escape detection. The weak absorption at 23200 cm^{-1} may be attributed to the second $^2T_{2g}$. One root of $^2T_{1g}$ (16612 cm^{-1}) is also found to be very close to the $^4T_{1g}$ (F) $\longrightarrow$ $^4T_{1g}$ (P) absorption band, while the second may be identified with the 18550 cm^{-1} band. The weak absorption at 20500 cm^{-1} has been assigned to $^4T_{1g}$ (F) $\longrightarrow$ $^2A_{1g}$ transition. The energy separation E(G) - E(F) is thus calculated to be 15385 cm^{-1}

B. Fine Features

As the 16000 cm^{-1} band is likely to be a superimposition of weak and strong transitions, we have investigated this band at liquid hydrogen temperature ($\simeq 20^0K$) under polarized light (Fig. 9a). The polarized spectrum of the spin-forbidden doublet $^2T_{1g}$ (^2H) in the region 18550 cm^{-1} has also been observed at 20^0K (Fig. 9b) under high dispersion. As the symmetry of $CoCl_6^=$ ions are not all perfectly octahedral, a part of these are in C_{3v} sites - the orbitals have been classified according to the symmetry properties of this subgroup. All the orbital triplets will split up into A and E terms under C_{3v} symmetry which in turn will give rise to E' and E" states (Griffiths notation)[41] under the effect of spin-orbit interaction. Using trigonal wavefunctions of Lehr[135] in the product form for $3d^7$, we have considered interactions between close-lying states $^4T_{1g}$ (P), $^2T_{2g}$

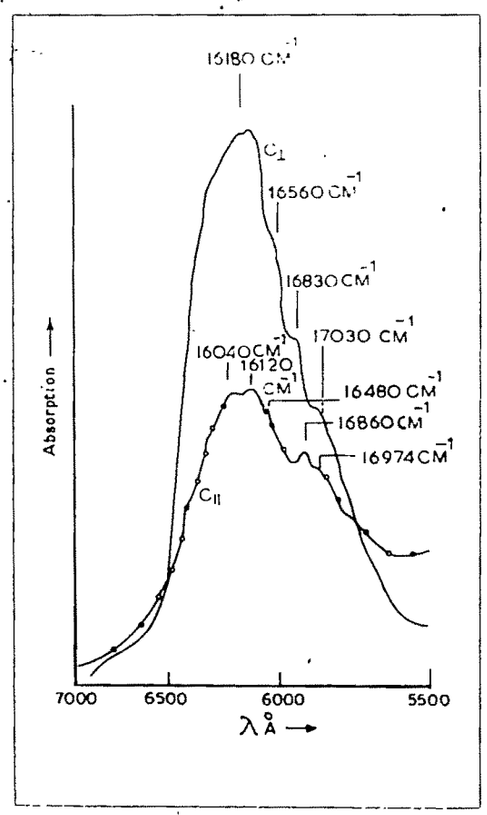

Fig.9a. Polarized absorption spectrum of $^4T_1$ (P) band of Co^{2+} in $CsCdCl_3$ at liquid hydrogen temperature (20°K).

Solid line - $C_\perp$

Chain line - $C_\parallel$

Fig.9a.

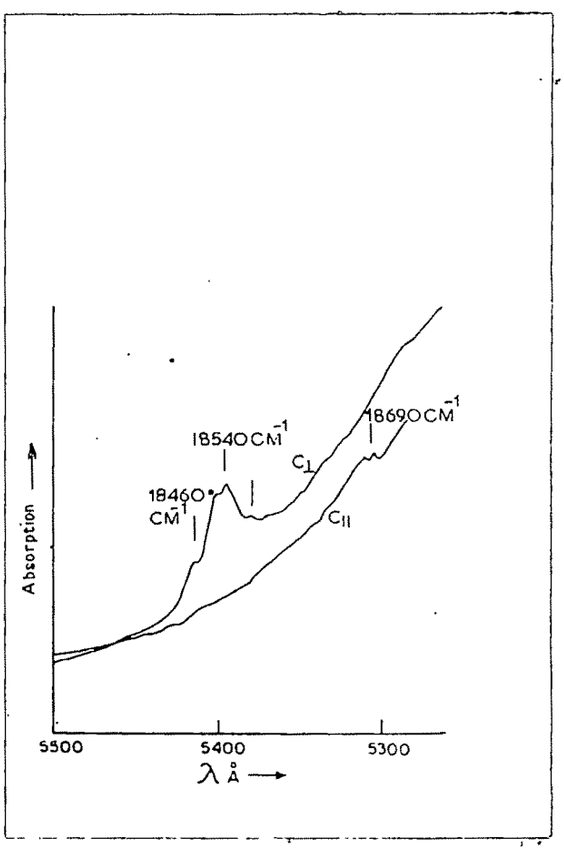

Fig.9b. Microphotometer tracings of high dispersion polarized spectrum of $^2T_1$ (H) band of $CsCdCl_3$: Co^{2+} at liquid hydrogen temperature (20°K).

Fig.9b.

$^2T_{1g}$ and $^2T_{1g}$ and solved 30 x 30 matrix, the perturbation Hamiltonian being $H' = V_{trig} + S.O.$ For convenience of our calculation, $^2A_{1g}$ and $^2T_{2g}$ terms which are far from above terms have been omitted. We varied trigonal field strength (Δ) from 150 cm^{-1} to 250 cm^{-1} at intervals of 10 cm^{-1} with reduced spin-orbit coupling constant $\zeta = 380 \pm 20$ cm^{-1} each time. Dq = 595 cm^{-1}, B = 800 cm^{-1} and C = 5B were used in the calculation. In order to find the energy of the lowest state, we have also solved 12 x 12 matrices of $^4T_{1g}$ (F) for same range of Δ and ζ. It was found that E' lies lowest. Fig. 10 shows the energy level scheme of the above terms under trigonal field and spin-orbit interaction. Polarization scheme from double groups are given in Table 10 to identify the levels. It is seen that if we consider Δ = 210 cm^{-1} and ζ = 380 cm^{-1}, our observed levels agree well with the calculated values (Table 11), except for a few cases.

Table 10 : Polarization scheme of Co^{2+} in C_{3v} using double groups

Transitions	Polarization	
	Z	(X,Y)
E' ⟶ E'	Allowed	Allowed
E' ⟶ E"	Forbidden	Allowed
E" ⟶ E"	Allowed	Forbidden

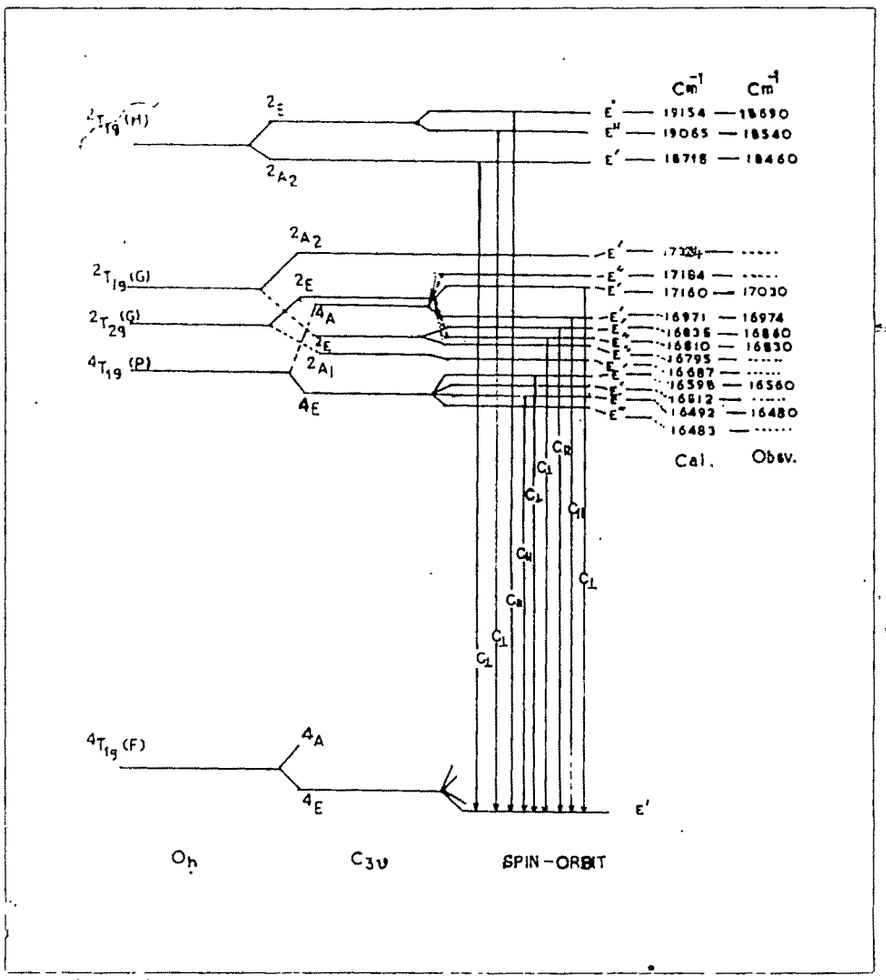

Fig.10. Fine structure energy level scheme of $^4T_1$ (P), $^2T_1$ and $^2T_2$ terms of Co^{2+} in $CsCdCl_3$. The energy levels were calculated assuming Dq = 595 cm^{-1}, B = 800 cm^{-1}, C = 513 cm^{-1} trigonal field parameter Δ = 210 cm^{-1} and ζ = 380 cm^{-1} (Not to scale).

Table 11 : Observed (under polarized light at 20^0K) and calculated (with Dq = 595 cm^{-1}, B = 800 cm^{-1}, C = 5B, Δ = 210 cm^{-1}, ζ = 380 cm^{-1}) fine structure energy levels of $^4T_1$ (P) and ^2T terms of $CsCdCl_3$: Co^{2+}. All are in cm^{-1}.

Term	Calculated	Observed*	Polarization	Transition
	16483	-		
	16492	16480	∥	E' ⟶ E'
	16512	-		
	16598	16560	⊥	E' ⟶ E'
$^4T_1$ (P)	16687	-		
	16795	-		
+ $^2T_2$ (G)	16810	16830	⊥	E' ⟶ E"
+ $^2T_1$ (G)	16835	16860	∥	E' ⟶ E'
	16971	16974	∥	E' ⟶ E'
	17160	17030	⊥	E' ⟶ E'
	17184	-		
	17324	-		
	18715	18460	⊥	E' ⟶ E'
$^2T_1$ (H)	19065	18540	⊥	E' ⟶ E"
	19154	18690	∥	E' ⟶ E'

* Some unpolarized bands were observed, which may be due to ions at O_h sites.

Comparison of our observed values with those of calculated levels shows that though the spin levels of $[{}^4T_1$ (P) + ${}^2_aT_2$ (G) + ${}^2_aT_1$ (G)] roughly agree with the calculated values, the agreement for ${}^2T_1$ (H) levels are not satisfactory. This may be due to the fact that we have neglected the interaction of the upper lying ${}^2_bT_2$ and ${}^2A_1$ states in our calculations. Their consideration would have lowered the calculated values of spin levels of ${}^2T_1$ (H), since all spin levels of ${}^2_bT_2$ and ${}^2A_1$, whose energies are higher than ${}^2T_1$ (H), will be of same symmetry (E' or E") as that of ${}^2T_1$ (H) and thus will depress the energies of spin levels of ${}^2T_1$ (H) bringing them nearer to our observed levels.

The small trigonal field (210 cm^{-1}) necessitated to interpret our polarized spectrum at 20°K are in good agreement with the axial field (200 cm^{-1}) needed to fit out magnetic data with the derived formula. The same is true for the spin-orbit coupling parameter ζ . Optically we have found out $\lambda_P = -\frac{1}{3}\zeta_{3d}$ = -126.6, and this should be equal to λ_F for $3d^7$ ion. The value of λ_F under the asymmetric crystal field obtained from magnetic measurements are : $\lambda_{\parallel} = -127$ cm^{-1} and $\lambda_{\perp} = -122$ cm^{-1}. However, in view of uncertainities in determination of parameters, too much reliance should not be placed on the exact agreement.

II. Magnetic Studies

Magnetic anisotropy and susceptibility was measured in the range 300°K to 90°K. Using experimental values of crystalline anisotropy and susceptibility and Eqn. (75) and (76)

we have calculated ionic values which are given in Table 12 at intervals of 20°K. The plot of ΔK_T vs T and $\bar{K}$ vs T are shown in Fig. 11a and Fig. 11b.

Table 12 : Magnetic susceptibility and anisotropy of $CsCd_{1-x}Co_xCl_3$ where x = 2.7 mol % (graphically interpolated values)

Temperature °K	$\chi_\perp \times 10^6$	$\Delta\chi \times 10^6$	$\Delta K \times 10^6$	$\bar{K} \times 10^6$
300	9890	566	850	10080
280	10887	638	957	11100
260	11730	810	1215	12000
240	12640	1056	1584	12980
220	13573	1570	2055	14030
200	14628	1755	2620	15210
180	15732	2273	3410	16490
160	17090	2850	4275	18040
140	18798	3525	5285	19970
120	21087	4390	6583	22450
100	24070	5490	8235	25900
90	25920	6078	9118	27950

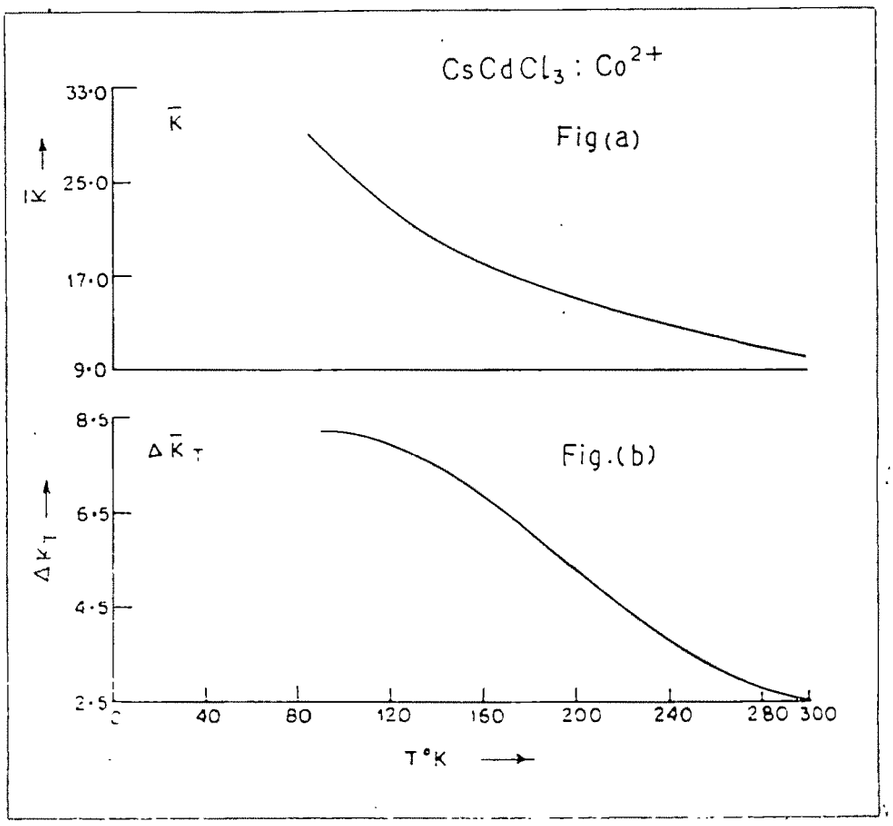

Fig.11

Fig.(a). Variation of mean susceptibility ($\bar{K}$) with temperature ($CsCdCl_3 : Co^{2+}$)

Fig.(b). Variation of $\Delta K.T$ with temperature ($CsCdCl_3 : Co^{2+}$)

A. Fine structure energy levels and magnetic susceptibility of trigonally distorted octahedral Co^{2+}

In calculating the fine structure energy levels of paramagnetic ion which have a degenerate ground state in a cubic field, Abragam and Pryce[9] took into consideration the effect of the upper orbital levels ($^4T_{2g}$, $^4A_{2g}$ and ^4P) on the ground triplet $^4T_{1g}$ (^4F). In order to incorporate the effect of the spin-orbit interaction and lower symmetry field on the lowest triplet, Abragam and Pryce introduced the fictitious orbital angular momentum $\bar{L}$ operating on the ground manifold with effective Lande factors $\alpha_{\parallel}$ and $\alpha_{\perp}$ in the axial and perpendicular directions. The states are designated by $m = (L'_z + S_z)$ values. Considering $^4T_{1g}$ as a "pseudoatomic" P-state, the basic orbitals are taken as

$$\begin{aligned} |1\rangle &= -\frac{1}{\sqrt{2}}(\phi'_x + i\phi'_y) \\ |0\rangle &= \phi'_z \\ |-1\rangle &= \frac{1}{\sqrt{2}}(\phi'_x - i\phi'_y) \end{aligned} \tag{79}$$

where $\phi'_i{}^{\Lambda}$, the linear combination of the ground state with the cubic $^4T_{2g}$ (Ψ's) and $^4A_{2g}$ (χ) as well as the ^4P (T) states are given as

$$\begin{aligned} \phi'_x &= \epsilon\phi_x - \tau\pi_x - \rho\Psi_y \\ \phi'_y &= \epsilon\phi_y - \tau\pi_y + \rho\Psi_x \\ \phi'_z &= \epsilon'\phi_z - \tau'\pi_z - \sigma\chi \end{aligned} \tag{80}$$

where ϵ'^{Λ}, τ'^{Λ}, ρ and σ are admixtural coefficient.

If the lower symmetry field splitting is denoted by Δ and the spin-orbit coupling by λ, then the Hamiltonian for the lowest orbital triplet can be written as

$$\mathcal{H}' = \Delta(1 - L_z'^2) - \alpha_{\parallel}\lambda L_z' S_z - \alpha_{\perp}\lambda(L_x' S_x + L_y' S_y) \qquad (81)$$

Operating with this Hamiltonian on the effective P-term, we get the matrices

$\underline{m = 1/2}$

	$\lvert 1, -1/2\rangle$	$\lvert 0, 1/2\rangle$	$\lvert -1, 3/2\rangle$
$\lvert 1, -1/2\rangle$	$(3/2)\alpha_{\parallel}\lambda$	$-\sqrt{3/2}\,\alpha_{\perp}\lambda$	0
$\lvert 0, 1/2\rangle$	$-\sqrt{3/2}\,\alpha_{\perp}\lambda$	Δ	$-\sqrt{2}\,\alpha_{\perp}\lambda$
$\lvert -1, 3/2\rangle$	0	$-\sqrt{2}\alpha_{\perp}\lambda$	$(1/2)\alpha_{\parallel}\lambda$

$\underline{m = 3/2}$

	$\lvert 1, 1/2\rangle$	$\lvert 0, 3/2\rangle$
$\lvert 1, 1/2\rangle$	Δ	$-\sqrt{3/2}\,\alpha_{\perp}'\lambda$
$\lvert 0, 3/2\rangle$	$-\sqrt{3/2}\,\alpha_{\perp}'\lambda$	$-(1/2)\,\alpha_{\parallel}'\lambda$

(83)

$\underline{m = 5/2}$

	$\lvert 1, 3/2\rangle$
$\lvert 1, 3/2\rangle$	$-(3/2)\alpha_{\parallel}'\lambda$

with identical matrices for m = -1/2, -3/2 and -5/2.

Uryû[141] and Bose et al[14] following Abragam and Pryce's method derived expressions for susceptibilities for

tetragonal and trigonal cases but without taking into consideration the overlap of charge clouds of metal and ligand orbitals. However, later on Bose et al[142] derived expressions for magnetic susceptibility and anisotropy of the trigonally distorted Co^{2+} complex taking into consideration the effect of the covalency overlap between the ligand s- and p-charge clouds and the central metal d-charge clouds. Due to anisotropic covalency overlap of the charge clouds they ihtroduced anisotropic reduction factor K_i ($i = 11^l$ or $\perp^r$) in the effective orbital moment and anisotropic spin-orbit coupling coefficient λ_i ($i = 11^l$ or $\perp^r$) in crystal.

With this refinement of the Hamiltonian (Eqn. 81) and calculating the effect of magnetic perturbations upto the second order, the principal magnetic susceptibilities K_{11} (K_z) and $K_\perp$ ($K_{x,y}$) for the trigonal case can be written as[142]

$$K_{11} = \frac{N\beta^2}{kz}\left[\frac{1}{T}\left\{\sum_{i=1,2\,6} G^i_{12}\exp\left(-\frac{E_i - E_1}{kT}\right) + \sum_{j=3,5} G^j_{12}\exp\left(-\frac{E_j - E_1}{kT}\right)\right.\right.$$

$$\left. + 2(3 - \alpha_{11}k_{11})^2\exp\left(-\frac{E_4 - E_1}{kT}\right)\right\} + 2k\left\{\sum_{\substack{i \\ i\neq l}}\sum_{l=1,2,6}\frac{S_{1l}}{E_l - E_i}\exp\left(-\frac{E_i - E_1}{kT}\right)\right.$$

$$\left.\left. + \frac{2}{E_5 - E_3}\left(3a_3a_5 - \alpha_{11}k_{11}b_3b_5 + b_3b_5\right)^2\left(\exp\left(-\frac{E_3 - E_1}{kT}\right) - \exp\left(-\frac{E_5 - E_1}{kT}\right)\right)\right\}\right] \quad (83)$$

K_{11} and $K_\perp$ stand for susceptibilities in 11^l & $\perp^r$ to c-axis respectively

k stands for Boltzman constant.

K_{11} and $K_\perp$ stand for orbital reduction factors in 11^l & $\perp^r$ to c-axis respectively.

$$K_{\perp} = \frac{N\beta^2}{kZ}\left[\frac{1}{T}\left\{\sum_{i=1,2,6} G_{1x}^{i}\exp\left(-\frac{E_i - E_1}{kT}\right)\right\} + 2k\left\{G_{2x}^{1} + G_{2x}^{2}\exp\left(-\frac{E_2 - E_1}{kT}\right)\right.\right.$$

$$+ G_{2x}^{3}\exp\left(-\frac{E_3 - E_1}{kT}\right) + G_{2x}^{4}\exp\left(-\frac{E_4 - E_1}{kT}\right)$$

$$\left.\left. + G_{2x}^{5}\exp\left(-\frac{E_5 - E_1}{kT}\right) + G_{2x}^{6}\exp\left(-\frac{E_6 - E_1}{kT}\right)\right\}\right] \qquad (84)$$

where G_1's and G_2's are the first and second order Zeeman terms, E_i, the energy of the ith level obtained by solving the secular matrices and Z, the partition function is given by $2\sum_{i=1}^{6}\exp\left(-\frac{E_i - E_1}{kT}\right)$ Explicit expressions for E_i's and G_1's are given below

$$E_1 = \alpha_{11}\lambda_{11}x_1$$

$$E_2 = \alpha_{11}\lambda_{11}x_2$$

$$E_3 = \frac{1}{2}\left[(\Delta - \tfrac{1}{2}\alpha_{11}\lambda_{11}) - \left\{(\Delta + \tfrac{1}{2}\alpha_{11}\lambda_{11})^2 + 6\alpha_{\perp}\lambda_{\perp}^2\right\}^{1/2}\right]$$

$$E_4 = -\frac{3}{2}\alpha_{11}\lambda_{11}$$

$$E_5 = \frac{1}{2}\left[(\Delta - \tfrac{1}{2}\alpha_{11}\lambda_{11}) + \left\{(\Delta + \tfrac{1}{2}\alpha_{11}\lambda_{11})^2 + 6\alpha_{\perp}^2\lambda_{\perp}^2\right\}^{1/2}\right]$$

$$E_6 = \alpha_{11}\lambda_{11}x_6$$

where x_1, x_2 and x_6 are the roots of the cubic equation

$$x^3 - x^2(2+\delta) + (2\delta + \frac{3}{4} - \frac{7}{2}\rho^2)x - \frac{3}{4}\delta + \frac{15}{4}\rho^2 = 0 \qquad (85)$$

where

$$\delta = \frac{\Delta}{\alpha_{11}\lambda_{11}}$$

$$\rho = \frac{\alpha_{\perp}\lambda_{\perp}}{\alpha_{11}\lambda_{11}} \qquad (86)$$

$$G^{i}_{1x} = \tfrac{1}{2}\left[\left\{2(a_i^2 - c_i^2)\alpha_{11}k_{11} + 6a_i^2 + 2b_i^2 - 2c_i^2\right\} + \left\{(3a_i^2 - c_i^2)\nu_1 + b_i^2\nu_2 + (\sqrt{6}\,a_i b_i - \sqrt{8}\,b_i c_i)\nu_3\right\}\right]^2$$

$$G^{j}_{1z} = 2\left[-b_j^2\alpha_{11}k_{11} + 3a_j^2 + b_j^2\right]^2$$

$$G^{i}_{1x} = \tfrac{1}{2}\left[\left\{-\frac{4\alpha_{\perp}k_{\perp}}{\sqrt{2}}b_i c_i + 4\sqrt{3}\,a_i c_i + 4b_i^2\right\} + \left\{b_i^2\nu_4 + c_i^2\nu_5 + \sqrt{3}\,a_i c_i\nu_6 + \sqrt{2}\,b_i c_i\nu_7\right\}\right]^2$$

$$G^{1}_{2x} = \sum_{l=2,6}\frac{t_{1l}}{E_l - E_1} + \sum_{j=3,5}\frac{u_{1j}}{E_j - E_1}$$

$$G^{2}_{2x} = \sum_{l=1,6}\frac{t_{2l}}{E_l - E_2} + \sum_{j=3,5}\frac{u_{2j}}{E_j - E_2} \qquad (87)$$

$$G^{3}_{2x} = \sum_{i=1,2,6}\frac{u_{i3}}{E_i - E_3} + \frac{v_3}{E_4 - E_3}$$

$$G^{4}_{2x} = \sum_{j=3,5}\frac{v_j}{E_j - E_4}$$

$$G^{5}_{2x} = \sum_{i=1,2,6} \frac{U_{i5}}{E_i - E_5} + \frac{V_5}{E_4 - E_5}$$

$$G^{6}_{2x} = \sum_{i=1,2} \frac{t_{i6}}{E_i - E_6} + \sum_{j=3,5} \frac{U_{6j}}{E_j - E_6}$$

$$S_{il} = 2\left[\alpha_{11} k_{11}(a_i a_l - c_i c_l) + (3 a_i a_l + b_i b_l - c_i c_l)\right]^2$$

$$t_{il} = 2\left[-\frac{\alpha_\perp k_\perp}{\sqrt{2}}(b_i c_l + b_l c_i) + (\sqrt{3} a_i c_l + 2 b_i b_l + \sqrt{3} a_l c_i)\right]^2$$

$$U_{ij} = 2\left[-\frac{\alpha_\perp k_\perp}{\sqrt{2}}(a_i a_j + b_i b_j) + (\sqrt{3} a_j b_i + 2 b_j c_i)\right]^2 \qquad (88)$$

$$v_j = 2\left[-\frac{\alpha_\perp k_\perp}{\sqrt{2}} a_j + \sqrt{3} b_j\right]^2$$

where a, b and c are the coefficients of the appropriate linear combinations of the basic functions used in the matrices (82a), (82b) and (82c) and are given by

$$a_i = \frac{\sqrt{\frac{3}{2}}\,\alpha_\perp \lambda_\perp}{\frac{3}{2}\alpha_{||}\lambda_{||} - E_i} b_i$$

$$c_i = \frac{\sqrt{2}\,\alpha_\perp \lambda_\perp}{\frac{1}{2}\alpha_{||}\lambda_{||} - E_i} b_i \qquad (89a)$$

with the normalizing condition $a_i^2 + b_i^2 + c_i^2 = 1$

and

$$a_j = \frac{\sqrt{\frac{3}{2}}\,\alpha_\perp \lambda_\perp}{\Delta - E_i} b_j \quad \text{with} \quad a_j^2 + b_j^2 = 1 \qquad (89b)$$

ν_i's are small terms arising from admixing the upper orbitals levels to ϕ (Defined by Eqn. 80) through spin orbit coupling and are given by Abragam and Pryce[9]. As $^4T_1$ (P) lies some 12000 cm^{-1} above ^4F, we have neglected ν's in Eqn. (87) in our calculations.

The g-values of the lowest Kramers doublet, for $||^l$ and $\perp^r$ directions of applied magnetic field are given by

$$g_{||} = 2\left\{\alpha_{||} K_{||} (a^2 - c^2) + 3a^2 + b^2 - c^2\right\}$$

$$g_\perp = 2\left\{-\sqrt{2}\, bc\alpha_\perp K_\perp + 2\sqrt{3}ac + 2b^2\right\} \qquad (90)$$

B. <u>Parametric Fittings and Disqussion of the Experimental Results</u>

From an inspection of the expressions of susceptibilities and g-values, it can be seen that these involve seven parameters, e.g. $\lambda_{||}$, $\lambda_\perp$, $K_{||}$, $K_\perp$, $\alpha_{||}$, $\alpha_\perp$ and the lower symmetry field parameter Δ .

After exhaustive trials we picked up a set of parameters which fits almost exactly to our experimental data at 100°K and gives closest approach to our experimental values at other temperatures. Calculated and experimental values of susceptibilities and anisotropies are given in Table 13. The data fitting at only five temperatures are shown in table as the temperature variation is smooth and continuous. The fine structure energy levels from our magnetic calculation are given in Fig. 11c.

Table 13 : Results of Parametric Fittings *

$\lambda_{\parallel} = -127\ cm^{-1}$		$\lambda_{\perp} = -122\ cm^{-1}$
$k_{\parallel} = 0.901$		$k_{\perp} = 0.786$
$\alpha_{\parallel} = 1.3$		$\alpha_{\perp} = 1.54$
$g_{\parallel} = 5.67$	$\Delta = +200\ cm^{-1}$	$g_{\perp} = 3.87$

Temperature °K	$\Delta K \times 10^6$	$\overline{K} \times 10^6$
300	792 (850)	10075 (10080)
250	1420 (1360)	12100 (12350)
200	2545 (2620)	14920 (15210)
150	4590 (4660)	19155 (19000)
100	8288 (8235)	26130 (25900)

* Values in parenthesis are the experimental values.

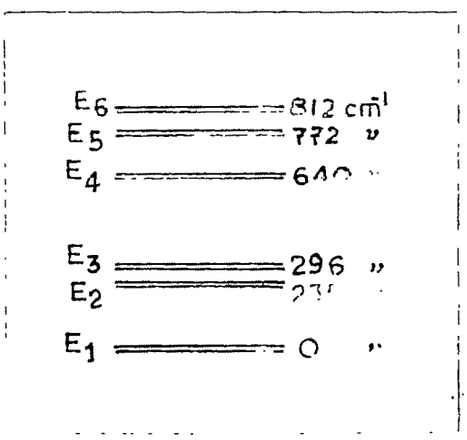

Fig.11c. Fine structure energy level scheme of ground $^4T_1$ (F) state of $CsCdCl_3 : Co^{2+}$ with Δ = +200 cm^{-1} from our magnetic calculation (Not to scale).

It can be seen from the table that there is systematic deviations as one goes up from 100°K towards 300°K. This is partly due to the fact that the above mentioned parameters, which fit exactly our experimental values at 100°K, are used to fit our values at other temperatures, which is not strictly correct. In selecting the values of the above parameters to explain our magnetic results, our optical observations made our task easier; the fact that nearly the same value of the parameters could explain both optical and magnetic results shows the essential soundness of both our optical and magnetic studies. Exact correlation between these two sets of data are not, however, possible owing to certain obvious approximations in the two sets of theoretical expressions as also owing to inherent difficulties in measuring techniques. The reduced anisotropic values of spin-orbit coupling constant; $\lambda_{\parallel} = -127$ cm^{-1} and $\lambda_{\perp} = -122$ cm^{-1}, in explaining our magnetic results is in good agreement with optical observation of λ_F ($\simeq$ 126.6 cm^{-1}). Anisotropic orbital reduction factors values of $k_{\parallel} = 0.901$ and $k_{\perp} = 0.786$ not only give further evidence of covalency overlap between the ligand and central metal charge clouds but also show its anisotropic nature. The value of the trigonal field splitting Δ (210 cm^{-1}) which can explain our polarized absorption spectrum at 20°K agrees well with that from our magnetic calculations (200 cm^{-1}). Moreover, the +ve sign of Δ showed that doublet E ~~lies lowest.~~ of ground state $^4T_1$ lies lowest.